

# Synthesis and Crystal Structures of Fluorinated Chromophores for Second-Order Nonlinear Optics

Hirohito Umezawa,<sup>\*1,†</sup> Shuji Okada,<sup>2</sup> Hidetoshi Oikawa,<sup>1</sup> Hiro Matsuda,<sup>3</sup> and Hachiro Nakanishi<sup>1</sup>

<sup>1</sup>Institute of Multidisciplinary Research for Advanced Materials, Tohoku University,  
2-1-1 Katahira, Aoba-ku, Sendai 980-8577

<sup>2</sup>Department of Polymer Science and Engineering, Faculty of Engineering, Yamagata University,  
4-3-16 Jonan, Yonezawa 992-8510

<sup>3</sup>National Institute of Advanced Industrial Science and Technology, Central 5, 1-1-4 Higashi, Tsukuba 305-8565

Received August 31, 2006; E-mail: umezawa@fukushima-nct.ac.jp

Partially fluorinated skeleton of 4-[2-(4-dimethylamino-2,3,5,6-tetrafluorophenyl)ethynyl]-2,3,5,6-tetrafluoro-*N,N,N*-trimethylanilinium (**2**) was synthesized as a second-order nonlinear optical (NLO) material to decrease the absorption around 1.3 and 1.5  $\mu\text{m}$ , which deteriorates the device efficiency. Several salts of **2** were prepared, and we found that the trifluoromethanesulfonate salt of **2** (**2b**) had a shorter absorption-maximum wavelength compared to that of 4-nitroaniline (pNA). From hyper-Rayleigh scattering (HRS) measurement, the  $\beta$  value of **2b** was found to be about 8 times greater than that of pNA. We also performed X-ray crystallographic analysis of **2b** and estimated NLO coefficient ( $d$ ) by the oriented gas model. We found that diagonal component of **2b** ( $d_{11} = 610 \text{ pm V}^{-1}$ ) was about 14 times greater than that of 2-methyl-4-nitroaniline and off-diagonal component of **2b** ( $d_{12} = 155 \text{ pm V}^{-1}$ ) was about 6.5 times greater than that of *N*-(4-nitrophenyl)-L-prolinol. Compound **2b** should be an excellent candidate for NLO applications.

A variety of organic chromophores for second-order nonlinear optical (NLO) materials have been studied over the last two decades,<sup>1–3</sup> because they have the potential to surpass inorganic materials. Especially, organic ionic chromophores have several advantages compared to non-ionic chromophores, like a large hyperpolarizability ( $\beta$ ), derived from charged  $\pi$ -conjugation systems, crystal structure controllability by changing the counter ion, and high melting points and hardness due to Coulombic interaction. However, most organic chromophores have C–H bonds, which cause absorption at wavelengths around 1.3 and 1.5  $\mu\text{m}$ , which are used for optical communications, due to overtones of C–H stretching vibration, limiting the performance in electro-optic (EO) applications. In this work, we investigated an ionic chromophore having C–F bonds instead of C–H bonds, since C–F bond shifts the absorption to lower energy. Sonoda et al. have synthesized deuterated compounds<sup>4–6</sup> for the same reason. However, shift range after C–D substitution is smaller than that after C–F substitution, because fluorine is heavier than deuterium. Thus, we tried to synthesize a chromophore with fluorine instead of hydrogen. In a previous study, we have synthesized 4-[2-(4-dimethylaminophenyl)ethynyl]-*N,N,N*-trimethylanilinium iodide (**1a**) (iodide salt of **1** as shown in Fig. 1). We have found that its  $\beta$  value is 7 times greater than 4-nitroaniline (pNA), which is traditionally used as a NLO material, in spite of having almost the same absorption region.<sup>7</sup> Therefore, we investigated fluorine substitution of the hydrogen atoms attached to the

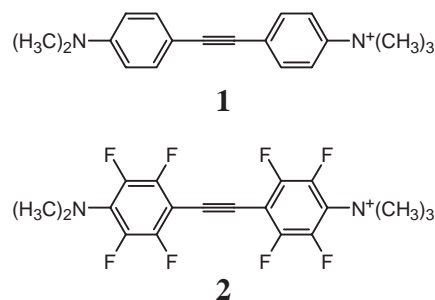


Fig. 1. Chemical structures of **1** and **2**.

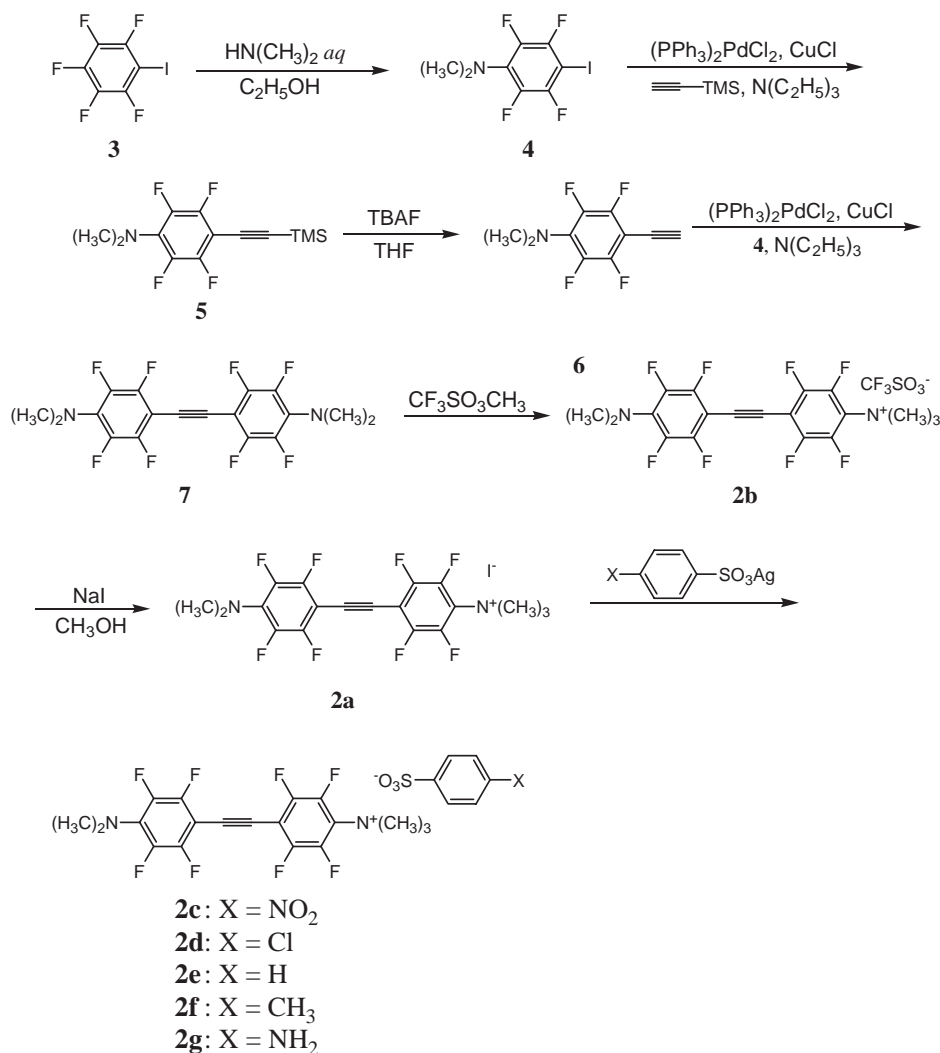
benzene rings of **1**. Namely, 4-[2-(4-dimethylamino-2,3,5,6-tetrafluorophenyl)ethynyl]-2,3,5,6-tetrafluoro-*N,N,N*-trimethylanilinium (**2**), as shown in Fig. 1, was synthesized, and its optical properties were studied.

## Experimental

Calculated  $\beta$  values ( $\beta_{0,\text{calc}}$ ), excitation energy ( $E_{\text{eg}}$ ), and dipole moment difference between the ground and excited states ( $\Delta\mu_{\text{eg}}$ ) of pNA, **1** and **2** were obtained by semiempirical molecular orbital (MO) calculations using MOPAC94 PM3 (CACHE ver. 4.1.1) on their optimized structure. Compound **2a** was synthesized according to Fig. 2. Experimental procedures are described below.

**2,3,5,6-Tetrafluoro-4-iodo-*N,N*-dimethylaniline (4).** To a mixture of pentafluoroiodobenzene (**3**) (47 g, 160 mmol) and ethanol (150 mL), 40% dimethylamine solution (45 mL) was added, and the solution was refluxed for 2 days. Then, the mixture was poured into water (300 mL) and extracted with ether (300 mL  $\times$  3). The organic phase was dried over  $\text{Na}_2\text{SO}_4$  and filtered. Solvent in the filtrate was removed under reduced pressure to give **4** as a

<sup>†</sup> Present address: Department of Chemistry and Biochemistry, Fukushima National College of Technology, 30 Aza Nagao Taira Kamiarakawa, Iwaki 970-8034

Fig. 2. Synthetic procedures for **2a** through **2g**.

yellow liquid (47 g, 92%). <sup>1</sup>H NMR (CDCl<sub>3</sub>, δ) 2.97 (t, *J* = 2.2 Hz, 6H); <sup>13</sup>C NMR (CDCl<sub>3</sub>, δ) 43.1 (t, *J*<sub>C-F</sub> = 4.3 Hz), 60.5 (t, *J*<sub>C-F</sub> = 27.9 Hz), 131.8 (tt, *J*<sub>C-F</sub> = 2.5, 10.5 Hz), 141.5 (dddd, *J*<sub>C-F</sub> = 4.6, 7.1, 13.9, 241 Hz), 147.4 (dddd, *J*<sub>C-F</sub> = 4.6, 7.1, 13.9, 241 Hz); Found: C, 30.04; H, 1.93; N, 4.18%. Calcd for C<sub>8</sub>H<sub>6</sub>F<sub>4</sub>IN: C, 30.12; H, 1.90; N, 4.39%.

**2,3,5,6-Tetrafluoro-4-trimethylsilylethynyl-*N,N*-dimethylaniline (5).** To a mixture of **4** (25 g, 78 mmol), dichlorobis(triphenylphosphine)palladium(II) (1.1 g, 1.6 mmol), CuCl (0.078 g, 0.79 mmol), and triethylamine (150 mL), trimethylsilylacetylene (15 mL) was added, and the mixture was stirred for 6 days at room temperature under a nitrogen atmosphere. Then, the mixture was filtered, and the solvent in the filtrate was removed under reduced pressure. The residue was purified by vacuum distillation (100–110 °C, 0.67 kPa) to give **5** (88 g, 71%) as pale-yellow liquid. <sup>1</sup>H NMR (CDCl<sub>3</sub>, δ) 0.27 (s, 9H), 2.99 (t, *J* = 2.4 Hz, 6H); <sup>13</sup>C NMR (CDCl<sub>3</sub>, δ) −0.2, 43.1 (t, *J*<sub>C-F</sub> = 4.6 Hz), 89.4 (t, *J*<sub>C-F</sub> = 3.7 Hz), 95.4 (tt, *J*<sub>C-F</sub> = 1.5, 18.5 Hz), 106.0 (t, *J*<sub>C-F</sub> = 3.5 Hz), 132.0 (tt, *J*<sub>C-F</sub> = 2.2, 11.1 Hz), 141.0 (dddd, *J*<sub>C-F</sub> = 3.9, 6.5, 13.4, 248 Hz), 147.8 (dddd, *J*<sub>C-F</sub> = 3.9, 6.5, 13.4, 248 Hz); Found: C, 53.94; H, 5.40; N, 4.64%. Calcd for C<sub>13</sub>H<sub>15</sub>F<sub>4</sub>NSi: C, 53.96; H, 5.23; N, 4.84%.

**4-Ethynyl-2,3,5,6-tetrafluoro-*N,N*-dimethylaniline (6).** To a

mixture of **5** (7.5 g, 26 mmol) and tetrahydrofuran (50 mL), 1 mol L<sup>−1</sup> tetrahydrofuran solution of tetrabutylammonium fluoride (52 mL) was added, and the mixture was stirred for 16 h. Then, concentrated hydrochloric acid (20 mL) and water (200 mL) were added, and the mixture was extracted with ether (150 mL × 3). The organic phase was dried over Na<sub>2</sub>SO<sub>4</sub> and filtered. Solvent in the filtrate was removed under reduced pressure to give **6** (6.0 g, 88%) as pale-yellow liquid. <sup>1</sup>H NMR (CDCl<sub>3</sub>, δ) 3.00 (t, *J* = 2.4 Hz, 6H), 3.50 (s, 1H); <sup>13</sup>C NMR (CDCl<sub>3</sub>, δ) 42.8 (t, *J*<sub>C-F</sub> = 4.3 Hz), 69.3 (t, *J*<sub>C-F</sub> = 3.6 Hz), 87.2 (t, *J*<sub>C-F</sub> = 3.4 Hz), 93.3 (t, *J*<sub>C-F</sub> = 18.3 Hz), 132.5 (tt, *J*<sub>C-F</sub> = 2.6, 10.4 Hz), 140.8 (dddd, *J*<sub>C-F</sub> = 4.2, 6.6, 12.7, 248 Hz), 148.0 (dddd, *J*<sub>C-F</sub> = 4.2, 6.6, 12.7, 248 Hz); Found: C, 55.81; H, 3.64; N, 5.84%. Calcd for C<sub>10</sub>H<sub>7</sub>F<sub>4</sub>N: C, 55.31; H, 3.25; N, 6.45%.

**4,4'-Ethynediylbis(2,3,5,6-tetrafluoro-*N,N*-dimethylaniline) (7).** To a mixture of **6** (10 g, 46 mmol), dichlorobis(triphenylphosphine)palladium(II) (0.64 g, 0.91 mmol), CuCl (0.046 g, 0.46 mmol), and triethylamine (150 mL), **4** (15 g, 47 mmol) was added, and the mixture was stirred for 3 days at room temperature under a nitrogen atmosphere. Then, the mixture was filtered, and solvent in the filtrate was removed under reduced pressure. The residue was recrystallized from chloroform to give **7** (7.0 g, 37%) as yellow crystals. Mp 195 °C; <sup>1</sup>H NMR (CDCl<sub>3</sub>, δ) 3.02

(*t*, *J* = 2.4 Hz, 12H);  $^{13}\text{C}$  NMR ( $\text{CDCl}_3$ ,  $\delta$ ) 43.1 (*t*,  $J_{\text{C-F}}$  = 4.8 Hz), 69.7 (*t*,  $J_{\text{C-F}}$  = 4.0 Hz), 82.6 (*t*,  $J_{\text{C-F}}$  = 4.0 Hz), 133.1 (*tt*,  $J_{\text{C-F}}$  = 2.2, 10.5 Hz), 140.5 (dddd,  $J_{\text{C-F}}$  = 4.1, 6.6, 13.6, 242 Hz), 148.6 (dddd,  $J_{\text{C-F}}$  = 4.1, 6.6, 13.6, 242 Hz); Found: C, 52.34; H, 2.99; N, 6.68%. Calcd for  $\text{C}_{18}\text{H}_{12}\text{F}_8\text{N}_2$ : C, 52.95; H, 2.96; N, 6.86%.

**4-[2-(4-Dimethylamino-2,3,5,6-tetrafluorophenyl)ethynyl]-2,3,5,6-tetrafluoro-*N,N,N*-trimethylanilinium Trifluoromethanesulfonate (2b).** A mixture of **7** (4.5 g, 11 mmol) and methyl trifluoromethanesulfonate (6.9 mL) were stirred for 2 days at room temperature. Then, chloroform was added, and the solution was filtered. The solid was washed with chloroform. After dissolving the remaining solid part using ethanol, the precipitate was filtered off. The solvent of the filtrate was removed under reduced pressure. The residue was recrystallized from methanol to give **2b** (3.5 g, 55%) as pale-yellow crystals. Mp 238 °C;  $^1\text{H}$  NMR ( $\text{CD}_3\text{OD}$ ,  $\delta$ ) 3.08 (*t*, *J* = 2.7 Hz, 6H), 3.94 (*t*, *J* = 1.8 Hz, 9H). Found: C, 41.52; H, 3.09; N, 5.14%. Calcd for  $\text{C}_{20}\text{H}_{15}\text{F}_{11}\text{N}_2\text{O}_3\text{S}$ : C, 41.97; H, 2.64; N, 4.89%. Unfortunately,  $^{13}\text{C}$  NMR data of **2b** could not be obtained because of the low solubility.

**4-[2-(4-Dimethylamino-2,3,5,6-tetrafluorophenyl)ethynyl]-2,3,5,6-tetrafluoro-*N,N,N*-trimethylanilinium Iodide (2a).** To a mixture of **2b** (3.5 g, 6.1 mmol) and methanol (100 mL), sodium iodide methanol solution (NaI 35 g, methanol 100 mL) was added. The mixture was stirred for a few seconds and poured into cold water (500 mL). The resulting precipitate was collected by filtration and washed with chloroform. After drying, **2a** was obtained as light-yellow powder (2.0 g, 60%). This compound was unstable and readily changed to **7**. So, we confirmed that this compound formed by the generation of silver iodide, by mixing it with a methanol solution of silver benzenesulfonate.

The melting points were determined by a differential scanning calorimeter (Perkin-Elmer Pyres Diamond DSC). The chemical structures of the compounds obtained were confirmed by  $^1\text{H}$  and  $^{13}\text{C}$  NMR spectroscopies (JEOL LAMBDA 400) and elemental analysis (IMRAM, Tohoku University). UV-visible absorption spectra were recorded on a Jasco V-570 spectrophotometer. IR spectra were recorded on a Nicolet AVATAR 360 spectrometer. Hyper-Rayleigh scattering (HRS) measurement<sup>21</sup> for **1a** and **2b** were performed by using a nano-second Nd:YAG laser (Coherent Infinity™ 40–100) at 1064 nm. These measurements were executed in methanol and pNA was used as an external standard,<sup>22</sup> of which the  $\beta$  value at 1064 nm in methanol is  $3.45 \times 10^{-29}$  esu. According to the two-level model,<sup>23</sup> the  $\beta$  values obtained were adjusted to  $\beta$  at zero frequency ( $\beta_{0,\text{exp}}$ ). The SHG activities of synthesized crystals were confirmed by the emission of green light (539.5 nm) after irradiation with a Nd:YAP laser (Elmas L-100) at  $\lambda = 1079$  nm. This was conducted only for qualitative purpose to remove the centrosymmetric crystals from further investigation. X-ray crystallographic analysis was performed using a Mac Science MXC3 diffractometer with a Mo  $K\alpha$  source ( $\lambda = 0.71073$  Å) for a crystal of **2b** grown in methanol solution by the slow evaporation method. Cell parameters were determined from 22 preliminary reflections. The crystal structure was determined by direct methods and refined by full-matrix least-squares procedures using the CRYSTAN program. Non-hydrogen atoms were refined anisotropically. Hydrogen atoms were attached to their parent atoms by fixed bond lengths and idealized bond angles and were refined isotropically. Crystallographic data have been deposited in Cambridge Crystallographic Data Centre as supplementary publication No. CCDC-255977. Copies of the data can be obtained free charge via <http://www.ccdc.cam.ac.uk/conts/retrieving.html> (or from the Cambridge Crystallographic Data

Table 1. Calculated  $E_{\text{eg}}$ ,  $\Delta\mu_{\text{eg}}$ , and  $\beta_0$  Values of pNA, **1**, and **2**

	$E_{\text{eg,calc}}/\text{eV}$	$\Delta\mu_{\text{eg}}/\text{Debye}$	$\beta_{0,\text{calc}}/10^{-30}$ esu
pNA	3.68	6.24	8.4
<b>1</b>	3.48	19.5	88.5
<b>2</b>	3.53	22.5	77.1

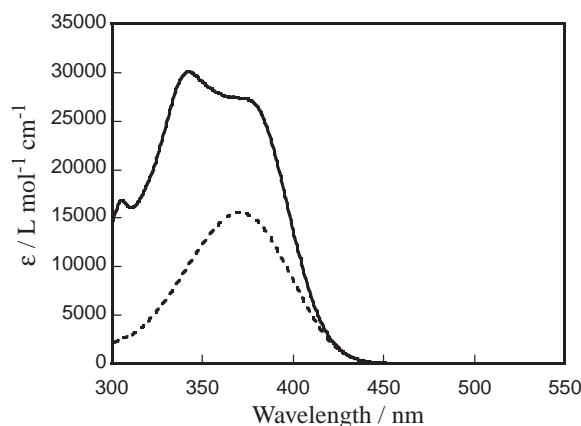


Fig. 3. UV and visible absorption spectra of **2b** (solid line) and pNA (dotted line) in methanol.

Centre, 12, Union Road, Cambridge, CB2 1EZ, UK; Fax: +44 1223 336033; or e-mail: [deposit@ccdc.cam.ac.uk](mailto:deposit@ccdc.cam.ac.uk)).

## Results and Discussion

MO calculations were performed on pNA, **1**, and **2** as shown in Table 1. The  $\beta_{0,\text{calc}}$  of **2** was estimated to be about 9 times greater than that of pNA, whereas the  $E_{\text{eg}}$  values were similar. The iodide salt of **2** (**2a**) was found to be unstable, and half of it was changed to **7** in a few days at room temperature. This is due to the relatively strong nucleophilicity of iodide anion compared to trifluoromethanesulfonate anion. An ammonio methyl group of **2a** is eliminated by nucleophilic attack of the iodide anion to give **7**, and the resulting methyl iodide evaporates. Then, in order to estimate the linear and nonlinear optical properties of cation **2**, **2b** was used instead of **2a**. The UV and visible absorption spectra of **2b** were measured in a methanol solution and compared with that of pNA. As shown in Fig. 3, absorption maximum wavelength ( $\lambda_{\text{max}}$ ) of **2b** was 342 nm, which is 27 nm shorter than that of pNA. However, absorption cutoff was almost the same, because **2b** had a shoulder at about 380 nm. In the solid state, the shoulder of **2b** disappeared, and the cutoff wavelength of **2b** was found to be shorter than that of pNA, as shown in Fig. 4. For  $\lambda_{\text{max}}$ , a similar tendency between two compounds was observed. The IR spectra of **2b** were also measured and compared with trifluoromethanesulfonate salt of **1** (**1b**) as shown in Fig. 5. Transmittances of **1b** and **2b** were normalized to each other in relation to the absorption around  $2200\text{ cm}^{-1}$ , which originates from stretching vibration of the  $\text{C}\equiv\text{C}$  bond. Absorption of C–H stretching vibration around  $3000\text{ cm}^{-1}$  of **2b** was found to be weakened compared to **1b**, because of the reduced number of C–H bonds in **2b**. Accordingly, lower absorption of **2b** around 1.3 and  $1.5\text{ }\mu\text{m}$  than **1b** was expected, since absorption around these wavelength regions is assigned to be overtones of C–H stretching vibration. Hyper-Rayleigh scatter-

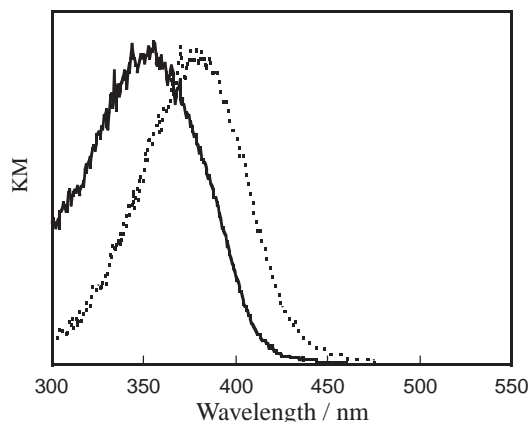


Fig. 4. UV and visible diffuse reflectance spectra of **2b** (solid line) and pNA (dotted line). Spectra were normalized at the maximum.

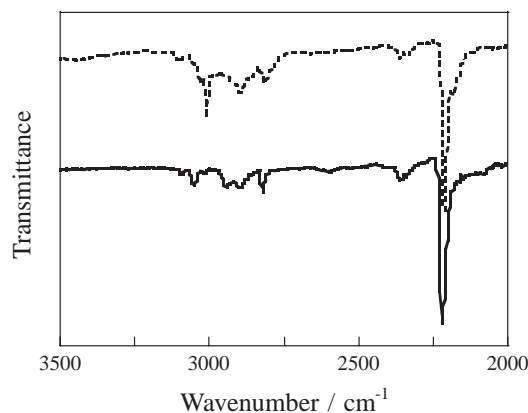


Fig. 5. IR spectra of **1b** (dotted line) and **2b** (solid line). Spectra were normalized using the absorption band around  $2200\text{ cm}^{-1}$ .

ing (HRS) measurement was performed on **2b** to clarify its molecular nonlinear optical efficiency. As shown in Fig. 6, quadratic dependence between fundamental and second-harmonic intensities was observed for **2b**. From fitted curves of the data, quadratic coefficients were obtained. The inset shows a linear plot of the quadratic coefficient as function of the ion-pair number density in the corresponding solution. By comparing these data to those for pNA as an external standard, the  $\beta$  value at  $1064\text{ nm}$  ( $\beta_{1064}$ ) of **2b** was determined to be  $234 \times 10^{-30}\text{ esu}$  and  $\beta_0$  was calculated to be  $123 \times 10^{-30}\text{ esu}$  from  $\beta_{1064}$  and  $\lambda_{\text{max}}$  by the two level model.<sup>23</sup> This  $\beta_0$  value is about 8 times greater than that of pNA. The counter anion of **2a** was changed to a 4-substituted benzenesulfonate (*p*-nitrobenzenesulfonate (**2c**), *p*-chlorobenzenesulfonate (**2d**), benzenesulfonate (**2e**), *p*-toluenesulfonate (**2f**), and *p*-aminobenzenesulfonate (**2g**)) to obtain the optimal crystals as studied before.<sup>8–12</sup> However, **2f** was unstable like **2a** for the same reason described above. By powder test of the prepared crystals, **2b**, **2c**, **2d**, and **2f** were found to have noncentrosymmetric structures. Single crystals of these four compounds were prepared by slow evaporation of respective methanol solutions under a nitrogen atmosphere. Good quality and reasonable size crystals were only obtained for **2b** so far. From the X-ray crys-

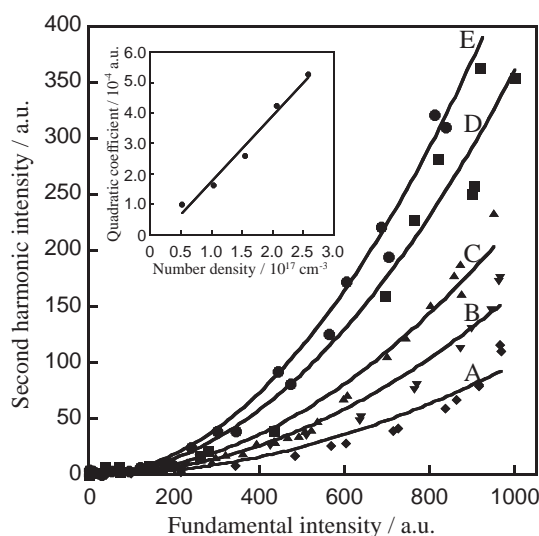


Fig. 6. The quadratic dependence between fundamental and second-harmonic intensities of **2b** in methanol at different ion-pair number densities: A,  $5.17 \times 10^{16}\text{ cm}^{-3}$ ; B,  $1.03 \times 10^{17}\text{ cm}^{-3}$ ; C,  $1.55 \times 10^{17}\text{ cm}^{-3}$ ; D,  $2.07 \times 10^{17}\text{ cm}^{-3}$ ; E,  $2.59 \times 10^{17}\text{ cm}^{-3}$ . Inset: the linear plot of the quadratic coefficient as function of the number density.

Table 2. Crystallographic Data of **2b**

Formula	$\text{C}_{20}\text{H}_{15}\text{F}_{11}\text{N}_2\text{O}_3\text{S}$
F.W.	572.4
Crystal system	Monoclinic
Space group	<i>Pc</i>
<i>a</i> /Å	8.093(2)
<i>b</i> /Å	11.155(3)
<i>c</i> /Å	14.255(7)
$\beta/^\circ$	117.4(1)
<i>V</i> /Å <sup>3</sup>	1142.4(9)
<i>Z</i>	2
$D_{\text{calcd}}/\text{Mg m}^{-3}$	1.728
$\mu (\text{Mo K}\alpha)/\text{mm}^{-1}$	2.474
No. of total reflections	2981
No. of unique reflections	2398
No. of reflections with $I > 2\sigma(I)$	1792
<i>R</i>	0.059
<i>wR</i>	0.052

tallographic analysis, the space group of the crystal of **2b** was found to be *Pc*, which is noncentrosymmetric, and the polar axis of this crystal was in *ac* plane. Details of crystallographic data and projection of the crystal structure are shown in Table 2 and Fig. 7, respectively. The angle between the polar axis and molecular long axis was found to be about  $14^\circ$ , if the molecular long axis was taken as a line linking two nitrogen atoms in the cation. Using this information, the second-order NLO coefficient (*d*) was estimated by using the oriented-gas model.<sup>13</sup> The local field factors of **2b** were set to be the same as those of a crystal of 4-[2-(4-dimethylaminophenyl)ethenyl]-1-methylpyridinium *p*-toluenesulfonate (DAST), which is a known organic ionic chromophore for second-order NLO material.<sup>14–16</sup> As a result, the diagonal component ( $d_{11}$ ) and off-diagonal component ( $d_{12}$ ) were estimated to be 610 and

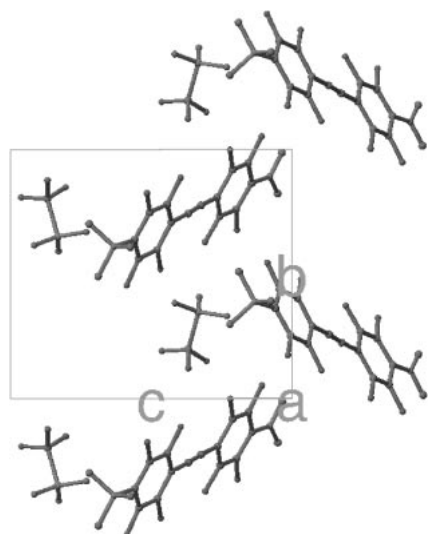


Fig. 7. Crystal structure of **2b** viewed along the *a* axis. Hydrogen atoms were omitted.

155 pm V<sup>-1</sup>, respectively. 2-Methyl-4-nitroaniline (MNA)<sup>17</sup> and *N*-(4-nitrophenyl)-L-prolinol (NPP)<sup>18–20</sup> are known to be typical second-order NLO materials, and they have a similar absorption to **2b**. Thus, the *d* values of these two crystals were also estimated by the same manner. MNA was found to have *d*<sub>11</sub> = 43.9 and *d*<sub>12</sub> = 21.8 pm V<sup>-1</sup> and NPP had *d*<sub>22</sub> = 8.9 and *d*<sub>21</sub> = 24.0 pm V<sup>-1</sup>. When the *d* values of **2b** were compared with those of MNA and NPP, **2b** was found to have 14 times greater diagonal component than that of MNA and 6.5 times greater off-diagonal component than that of NPP. These results are caused by the large  $\beta$  value, which represents microscopic efficiency, and efficient cation alignment in the crystal of **2b** compared with MNA and NPP.

In conclusion, we successfully synthesized the partially fluorinated skeleton **2**. From the UV and visible absorption spectrum,  $\lambda_{\text{max}}$  of **2b** was shorter than that of pNA, while the  $\beta_0$  value was about 8 times larger. In the IR spectra, absorption originated from C–H stretching vibration of **2b** was less intense than that of **1b**. Therefore, **2b** should have a lower absorption around 1.3 and 1.5  $\mu\text{m}$ , where overtones of C–H stretching vibration are most prominent, compared with **1b**. By using the oriented-gas model, the diagonal *d* component of **2b** was estimated to be 14 times greater than that of MNA, and the off-diagonal *d* component was estimated to be 6.5 times greater than that of NPP. From these results, we think that **2b** is an excellent candidate for second-order NLO device applications. Since deuteration of hydrogen in methyl group is not so difficult task and generally does not change the crystal structure of a compound,<sup>24</sup> the corresponding chromophore without C–H bonds is being synthesized and investigated.

## References

- 1 *Nonlinear Optical Properties of Organic and Polymeric Materials*, ed. by D. J. Williams, ACS Symp. Ser., 233, American Chemical Society, Washington, D. C., **1983**.
- 2 C. Bosshard, K. Sutter, P. Prêtre, J. Hulliger, M. Flörsheimer, P. Kaatz, P. Günter, *Organic Nonlinear Optical Materials in Advances in Nonlinear Optics*, Gordon and Breach Publishers, Basel, **1995**, Vol. 1.
- 3 *Nonlinear Optics of Organic Molecules and Polymers*, ed. by H. S. Nalwa, S. Miyata, CRC Press, Boca Raton, **1997**.
- 4 H. Minemoto, Y. Ozaki, N. Sonoda, *J. Appl. Phys.* **1994**, 76, 3975.
- 5 H. Minemoto, Y. Ozaki, N. Sonoda, *Appl. Phys. Lett.* **1993**, 63, 3565.
- 6 A. Yokotani, T. Sasaki, K. Fujioka, S. Nakai, C. Yamanaka, *J. Cryst. Growth* **1990**, 99, 815.
- 7 H. Umezawa, S. Okada, H. Oikawa, H. Matsuda, H. Nakanishi, *J. Phys. Org. Chem.* **2005**, 18, 468.
- 8 K. Nogi, Anwar, K. Tsuji, X.-M. Duan, S. Okada, H. Oikawa, H. Matsuda, H. Nakanishi, *Nonlinear Opt.* **2000**, 24, 35.
- 9 H. Umezawa, K. Tsuji, Anwar, X.-M. Duan, S. Okada, H. Oikawa, H. Matsuda, H. Nakanishi, *Nonlinear Opt.* **2000**, 24, 73.
- 10 S. Okada, K. Tsuji, Anwar, H. Nakanishi, H. Oikawa, H. Matsuda, *Nonlinear Opt.* **2000**, 25, 45.
- 11 H. Umezawa, K. Tsuji, S. Okada, H. Oikawa, H. Matsuda, H. Nakanishi, *Opt. Mater.* **2002**, 21, 7578.
- 12 H. Umezawa, S. Okada, H. Oikawa, H. Matsuda, H. Nakanishi, *Bull. Chem. Soc. Jpn.* **2005**, 78, 344.
- 13 J. Zyss, J. L. Oudar, *Phys. Rev. A* **1982**, 26, 2028.
- 14 S. Okada, H. Matsuda, H. Nakanishi, M. Kato, R. Muramatsu, Japanese Patent Application 61-192404, **1986**; S. Okada, H. Matsuda, H. Nakanishi, M. Kato, R. Muramatsu, Japanese Patent 1716929, **1992**.
- 15 H. Nakanishi, H. Matsuda, S. Okada, M. Kato, *Mater. Res. Soc. Int. Mtg. Adv. Mater.* **1989**, 1, 97.
- 16 S. R. Marder, J. W. Perry, W. P. Schaefer, *Science* **1989**, 245, 626.
- 17 B. F. Levine, C. G. Bethea, C. D. Thurmond, R. T. Lynch, J. L. Bernstein, *J. Appl. Phys.* **1979**, 50, 2523.
- 18 I. Ledoux, D. Josse, P. Vidakovic, J. Zyss, *Opt. Eng.* **1986**, 25, 202.
- 19 J. Zyss, J. F. Nicoud, M. Coquillay, *J. Chem. Phys. Lett.* **1977**, 48, 2669.
- 20 J. Zyss, *J. Phys. D: Appl. Phys.* **1993**, 26, B198.
- 21 K. Clays, A. Persoons, *Phys. Rev. Lett.* **1991**, 66, 2980.
- 22 M. A. Pauley, H.-W. Guan, C. H. Wang, A. K.-Y. Jen, *J. Chem. Phys.* **1996**, 104, 7821.
- 23 J. L. Oudar, D. S. Chemla, *J. Chem. Phys.* **1977**, 66, 2664.
- 24 Z. Glavcheva, H. Umezawa, Y. Mineno, T. Odani, S. Okada, S. Ikeda, T. Taniuchi, H. Nakanishi, *Jpn. J. Appl. Phys.* **2005**, 44, 5231.